Variable Pulse Duration Laser for Material Processing

Werner Wiechmann, Loren Eyres, James Morehead, Jeffrey Gregg, Derek Richard, Will Grossman

JDSU Corporation, 430 North McCarthy Boulevard, Milpitas, CA 95035, U.S.A.
E-mail: Werner.Wiechmann@jdsu.com

We have developed a means to electronically tune laser pulse durations and achieve nearly constant, stable output power. This technique may be used to obtain variable pulse durations and peak powers at a constant pulse repetition rate, or constant pulse durations over a range of pulse repetition rates. These new capabilities allow great flexibility for material processing applications, making it possible to tailor and optimize the performance of a single laser for a wide variety of applications. We report development of next-generation Q-switched, intra-cavity frequency-converted, diode-pumped, near diffraction-limited Nd:YAG lasers with output powers of 30 W at 355 nm and 40 W at 532 nm. Operating at 532 nm we have demonstrated a variable pulse width externally adjustable over the range of 40 ns to 300 ns at constant pulse repetition rates.
DOI: 10.2961/jlmn.2007.01.0012

Keywords: Diode-pumped solid-state lasers, Nd:YAG, Q-switching, frequency conversion, variable pulse width, stability, gain insensitivity

1. Introduction

Multi-watt frequency-converted high repetition rate, diode-pumped solid-state Q-switched lasers with near-diffraction-limited TEM_{00} beams have proven their usefulness in various high-precision micromachining applications within the microelectronics industry. These applications include UV micro via drilling, low-k dielectric grooving, thin-wafer drilling and dicing, and wafer scribing [1]. In each of these applications the laser has provided the enabling technology for miniaturization and higher feature integration.

Most lasers employed in the above mentioned applications are diode-pumped Q-switched Nd:YAG or Nd:YVO_4 lasers that are frequency-converted from 1064 nm to 532 nm (SHG) or to 355 nm (THG). Here, the shorter wavelength enables a smaller spot size at a given working distance and a material interaction with shorter absorption depth and a significantly reduced heat-affected zone.

There are two approaches to harmonic generation – intra-cavity and extra-cavity frequency conversion. Both approaches have their advantages and disadvantages. Intra-cavity harmonic lasers are able to convert the fundamental wavelength extremely efficiently to the harmonic output with very low pulse-to-pulse fluctuations, while extra-cavity harmonic lasers enable a more modular approach to harmonic generation that lends itself more easily to shorter pulse durations, but suffer from larger pulse-to-pulse fluctuations.

2 Noise in frequency-converted lasers

Noise characteristics of frequency-converted lasers and lasers in general are critical for micromachining applications. This is true in particular for single pulse processes such as link blowing or for line applications with only partial pulse overlap such as solar cell or low-k dielectric scribing. There are several sources of noise such as noise coupled through the pump diodes and the Q-switch control and drive circuitry or noise from externally coupled mechanical vibrations. Noise may also arise from parasitic higher order transverse modes or parasitic non-axial modes around the gain medium that may use the same stored energy as the fundamental resonator mode. Another important source of noise is the interference of a multitude of longitudinal modes oscillating simultaneously in the laser resonator. Figure 1 depicts such mode beating of an intra-cavity frequency-converted 355-nm laser. The red curve represents the IR pulse measured with a high-speed photo detector while the blue curve represents the time averaged 355nm pulse. A spectral analysis of the IR photo detector signal reveals simultaneous oscillation of more than 20 longitudinal modes.

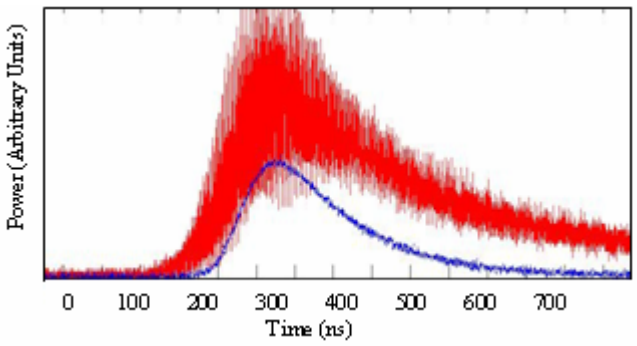

Figure 1: IR measured with high-speed photo detector (red curve); the lower blue curve indicates the time-averaged 355-nm pulse.

The pulse-to-pulse noise of the harmonic output may be the result of the random nature of the modulation depth of the mode beating and its effect on the time-averaged conversion efficiency. For example, when neglecting saturation effects a pulse with a 100 % sinusoidal modulation depth frequency-converts approximately 1.5 times more efficiently to the second harmonic than the same pulse with no mode beating. In [2] it is shown that the pulse-to-pulse stability of intra-cavity frequency-converted lasers suffers significantly less from the random nature of longitudinal mode beating since the intra-cavity fundamental average

power decreases as the modulation depth and hence the conversion efficiency is increased. This self-stabilizing effect results from the fact that the loss of intra-cavity frequency-converted lasers is dominated by the nonlinear loss from the frequency conversion process itself.

3 Pulse width of frequency converted lasers

Another important aspect of frequency-converted lasers is the temporal profile of the laser pulse. While some micromachining applications may not place stringent requirements on the pulse width and pulse peak power, the ablation characteristics of other applications may depend critically on these parameters. Some applications require short pulses with high pulse peak powers while other applications demand long pulses with low peak powers. Many micromachining applications involve multiple materials and process steps and it might be desirable to employ short pulse widths for one process step while other process steps may be better performed with longer pulses.

As mentioned above, extra-cavity harmonic lasers provide more flexibility when it comes to tailoring the pulse width to a particular application. In particular, extra-cavity harmonic lasers enable generation of shorter pulses because it is easier to tailor the length of the fundamental resonator and the output coupling to obtain the desired pulse width.

On the contrary, intra-cavity frequency-converted lasers are designed for a minimum linear loss and the output coupling is provided by the nonlinear frequency conversion process. In other words, the intra-cavity frequency-converted laser trades the fixed output coupler for a nonlinear output coupler. As the laser pulse builds up inside the resonator, the output coupling increases rapidly until the increasing nonlinear loss limits the intra-cavity intensity. As the pulse decays, the output coupling decreases and the pulse is stretched out. Hence, internally frequency-converted lasers typically exhibit longer pulses than lasers that employ external frequency conversion.

3.1 Pulse shortening by means of pulse clipping

As mentioned above, the ideal laser may provide pulse widths that are easily adjustable for different processes or process steps. One technique for controlling the pulse width of a Q-switched laser is the use of a low-loss Q-switch window that terminates prior to the conclusion of the natural pulse set by the gain and energy extraction dynamics of the laser cavity [3]. Here, the Q-switch rapidly reduces the circulating intensity within the tail of the laser pulse. When the pulse repetition rate is low compared to the inverse of the upper state lifetime, this pulse-clipping technique can shorten pulses effectively. However, the clipping of the pulse reduces the overall output power since the stored energy left behind after the termination of the laser pulse will have decayed prior to the initiation of the next laser pulse and hence goes to waste.

At repetition rates that are large compared to the inverse of the upper state lifetime the left-over energy does not have enough time to decay and is largely available for the next pulse. However, as the low-loss Q-switch window is decreased more, the left behind gain may provide a mechanism for communication between pulses which may destabilize the pulse train.

3.1.1 Pulse-train instability due to pulse clipping

The above described instability may be explained by considering the two coupled equations for circulating power P and gain g in a linear laser in the high pulse repetition rate limit:

$$T_{RT}\frac{dP}{dt} = (g - l)P \qquad (1)$$

$$\frac{dg}{dt} = -gP / E_{sat} \qquad (2)$$

Here, E_{sat} depicts the gain medium saturation energy, T_{RT} is the cavity round trip time and l represents the cavity loss. We assume that the pulse is sufficiently short and repumping of the gain medium during the pulse can be ignored.

Figure 2 shows two numerical solutions of the above equations for two slightly different initial gain values. The third graph shows the gain difference between both solutions.

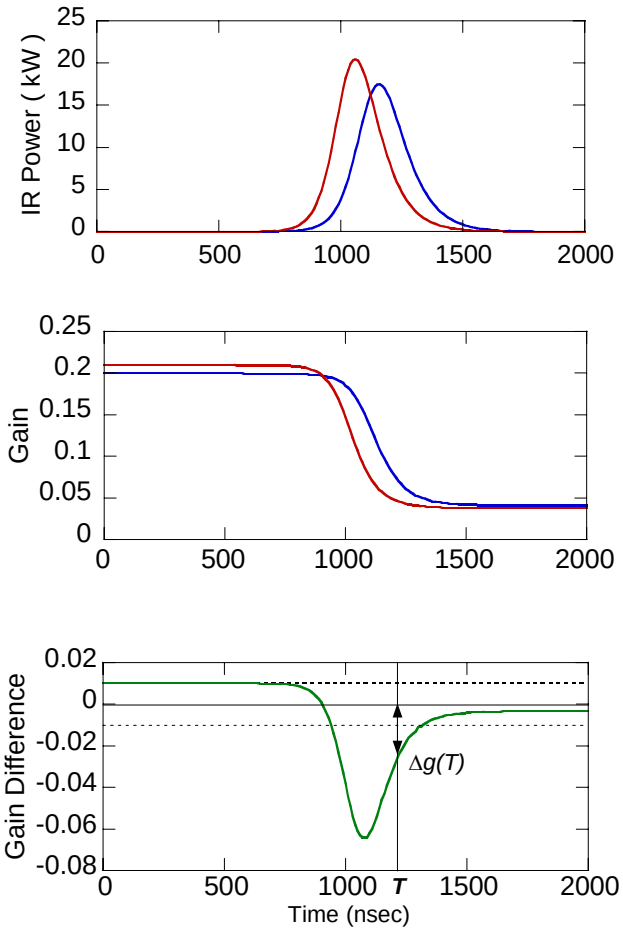

Figure 2: Circulating IR power, gain and gain difference versus time for two initial gain conditions.

The initial gain difference remains almost constant through the pulse build-up phase, but once significant energy extraction begins, a much larger difference in gain exists for most of the pulse duration. After the circulating intensity has decayed, the instantaneous gain difference drops to a value lower than the initial gain difference at time t=0. If the Q-switch were turned back to a high loss state at time T,

we can infer the impact on stability by comparing the gain difference at time T "$\Delta g(T)$" to the initial gain difference "$\Delta g(0)$". The pulse train will be stable if the following minimum condition is satisfied:

$$|\Delta g(T)/\Delta g(0)| < 1 \qquad (3)$$

From Figure 2 it is clear that this condition is violated when the low-loss Q-switch window is shortened such that T begins to encroach on the falling edge of the pulse. Under this condition any gain fluctuations will be amplified in their effect on subsequent pulses. This maybe understood intuitively as follows: Extra gain is available for a pulse which builds up faster and extracts more stored energy, leaving less stored energy for the next pulse. Hence, this pulse is building up more slowly and extracts less energy, leaving more stored energy for the next pulse. This pattern is repeated as long as condition 3 is violated.
Figure 3 shows the results of numerical simulations of the impact of the Q-switch timing on pulse width in a laser prone to this instability. As the low-loss Q-switch window is shortened and begins to clip the falling edge of the pulse, a bifurcation in pulse energy and pulse width occurs such that the pulse train contains alternating large and small pulses. As the window is closed further, the energy of the smaller pulse quickly goes to zero, so that the laser reaches threshold only on alternating Q-switch events and the repetition rate is cut in half.

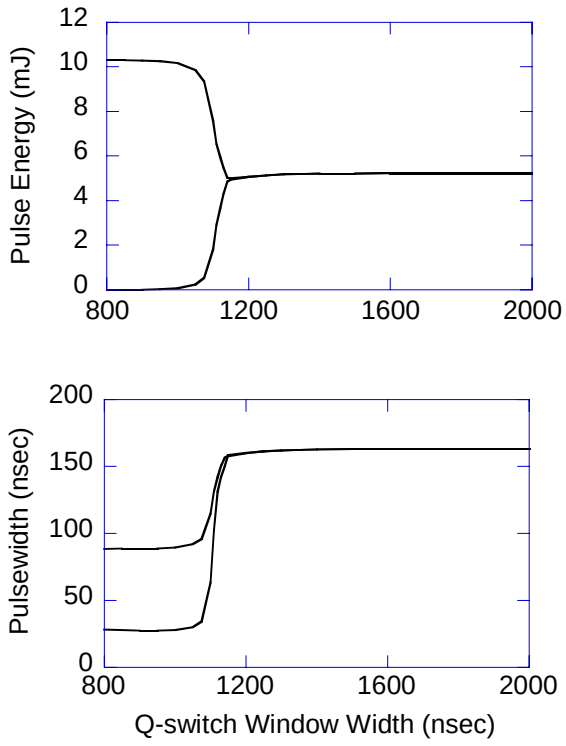

Figure 3: Pulse energy and pulse width versus Q-switch window width illustrating pulse instability and bifurcation.

3.1.2 Gain insensitivity and pulse-train stabilization

In intra-cavity frequency-converted lasers it is possible to reduce the pulse width by pulse clipping without suffering from the above described destabilization of the pulse train [3]. This is accomplished by choosing the nonlinear coupling α such that the gain during the pulse decay is independent of the initial gain condition.
For an intra-cavity frequency-converted laser Equations 1 and 2 may be substituted by:

$$T_{RT}\frac{dP}{dt} = gP - \alpha P^2 \qquad (4)$$

$$\frac{dg}{dt} = -\frac{gP}{E_{sat}} \qquad (5)$$

Here, the linear loss l is neglected.
In [3] it is shown that the nonlinear coupling for gain independence is a function of the cavity roundtrip time, the saturation energy, the pulse peak power P_p and the initial power circulating in the cavity prior to opening of the Q-switch $P_{initial}$:

$$\alpha_{\text{gain independence}} \approx \frac{T_{RT}}{E_{sat}}\left[\ln\left(P_p / P_{initial}\right) - 1\right] \qquad (6)$$

It is also shown that this coupling is many times larger than the optimum nonlinear output coupling $\alpha \approx T_{RT}/E_{sat}$ for highest harmonic peak power, near-maximum efficiency and near-minimum pulse width as determined by Murray and Harris [4]. As a result, without pulse clipping the pulse width of the gain-insensitive laser will be significantly longer than the pulse width of the same laser with optimum nonlinear coupling. However, because of the enhanced pulse train stability, the gain-insensitive laser will now allow Q-switch clipping to achieve shorter pulses and higher peak powers.
Figure 4 shows the numerical simulation of the coupled Equations 4 and 5 with a gain-independent nonlinear coupling value α of approximately 0.038/kW.

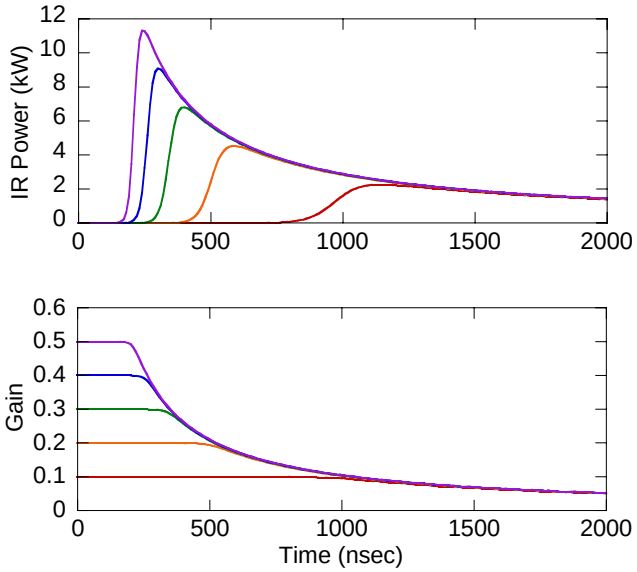

Figure 4: Circulating IR power and gain vs. time for a gain-independent nonlinear coupling value.

Here, all gain curves merge into a single curve immediately following the peak of the pulse, independent of the initial

gain condition. Hence, even with pulse clipping $\Delta g(T)$ is zero or close to zero and the pulse train remains stable.

4. Next generation high-power Q-switched intra-cavity harmonic lasers

In the following we describe two next-generation high-power intra-cavity frequency-converted Q-switched lasers, one operating at 532 nm and the other operating at 355 nm. Figures 5 and 6 show the principal resonator layouts.

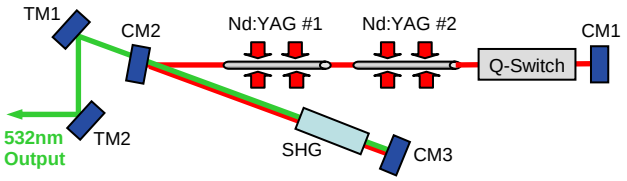

Figure 5: Principal resonator layout of the 532nm laser.

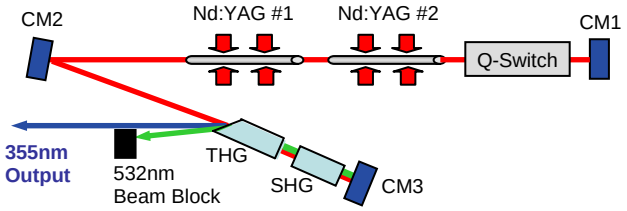

Figure 6: Principal resonator layout of the 355nm laser.

Both lasers employ two of JDSU's Direct-Coupled Pump (*DCP*®) modules. In this architecture the pump diodes are closely coupled to a Nd:YAG rod without beam shaping optics and the pump light is confined within the pump volume through a reflective surface [5]. The total 808-nm pump power is 240 W. The resonator is folded with a total round trip time of approximately 5 ns and effective saturation energy of approximately 3 mJ. All cavity mirrors CM1-CM3 are coated for high reflectivity at 1064 nm and thermally-induced depolarization loss is minimized by employing a proprietary compensation scheme. The Q-switch consists of an acousto-optic modulator whose low-loss RF window is electronically controlled via an externally applied TTL trigger signal.

4.1 SHG laser

For the SHG laser, a 20 mm long LBO crystal cut for Type I phase-matching and 1064-to-532 nm conversion provides a nonlinear coupling of approximately 0.04/kW. Note that this is close to the above discussed nonlinear coupling for gain independence.

Figure 7 shows the average power and the pulse width at a pulse repetition rate of 100 kHz as a function of the RF window length while Figure 8 illustrates the temporal shapes of the pulses when the RF window is 0.25, 0.4, 1.0 and 3.0 µs. Note that the vertical scale is adjusted to accommodate the growing pulse peak as the RF window length is shortened and the pulses are increasingly truncated. At an RF window length of 0.4 µs and less the pulse tail is almost entirely eliminated and the pulses develop a very sharp peak. The average power is more than 40 W at an RF window length of 0.8 µs and the power decreases to 30 W as the RF window is shortened to 0.3 µs. Using this method, we were able to tune the pulse within the range of 40 to 300 ns.

Throughout the measurements the pulses remained stable without any signs of bifurcation which is attributed to the high nonlinear coupling.

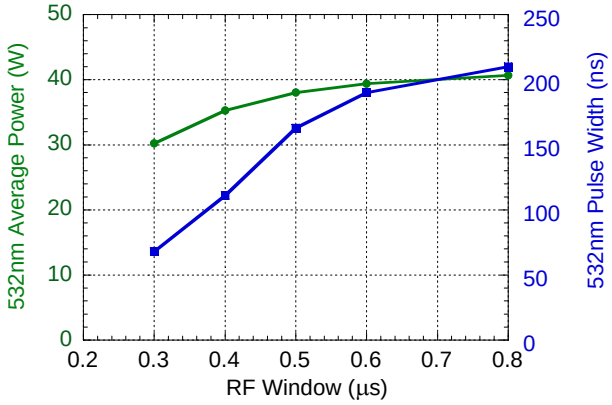

Figure 7: 532-nm average power and pulse width as a function of RF window length at a pulse repetition rate of 100 kHz.

4.2 THG laser

For the THG laser we shortened the SHG LBO crystal to 5 mm and inserted a 20 mm LBO crystal cut for Type II phase-matching from 1064 and 532 nm to 355 nm. The effective nonlinear SHG coupling is 0.004/kW which is significantly less than the value calculated for gain independence. Note that the UV output face of the THG crystal is cut at Brewster's angle at the fundamental 1064 nm wavelength [6]. This enables prism-like beam separation and eliminates any coatings within the p-polarized 355-nm beam path.

Figure 9 shows the UV output power and pulse width as a function of pulse repetition rates. The RF window is optimized to yield the highest average power without evoking the pulse instabilities discussed above. The peak-to-peak noise is measured as <±5 % at 100 kHz. The maximum average 355 nm output power is 30 W at a pulse repetition rate of 50 kHz. This corresponds to a 12.5 % optical-to-optical efficiency (pump diode output to 355-nm output).

5. Conclusion

We discussed noise characteristics of intra-cavity and extra-cavity frequency-converted lasers. We also determined a method of electronically tuning the pulse width of intra-cavity frequency-converted lasers and demonstrated this method within a next-generation 40-W frequency doubled Q-switched laser. Lastly, we described a next-generation 355-nm laser with up to 30 W output. Both lasers are expected to prove their usefulness in various high-precision materials processing applications.

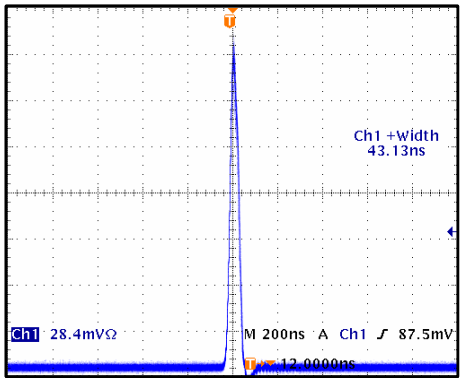

(a) RF window: 0.25μs; pulse width: 43ns

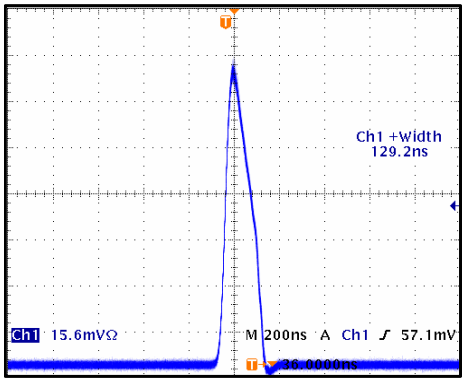

(b) RF window: 0.4μs; pulse width: 129ns

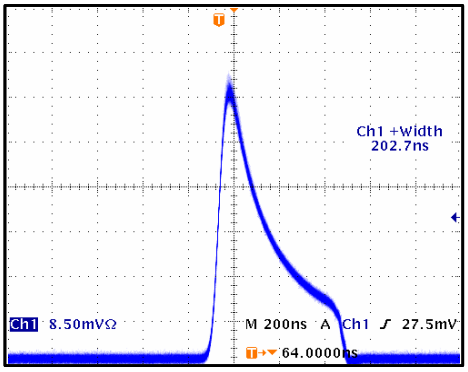

(c) RF window: 1.0μs; pulse width: 203ns

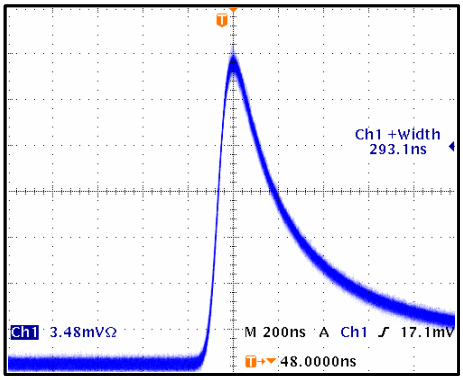

(d) RF window: 3.0μs; pulse width: 293ns

Figure 8 (a)-(d): Laser pulse shape at different RF window lengths; the vertical axis is scaled to the peak height for each pulse.

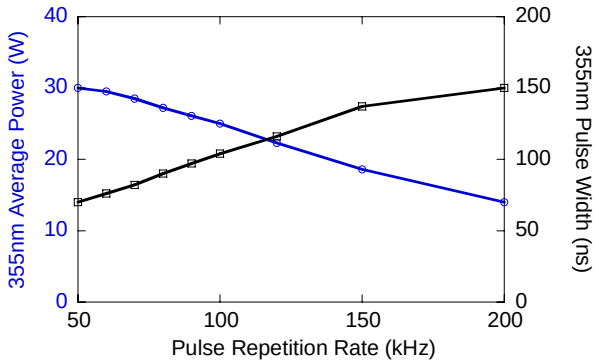

Figure 9: Average 355-nm power and pulse width as a function of pulse repetition rate.

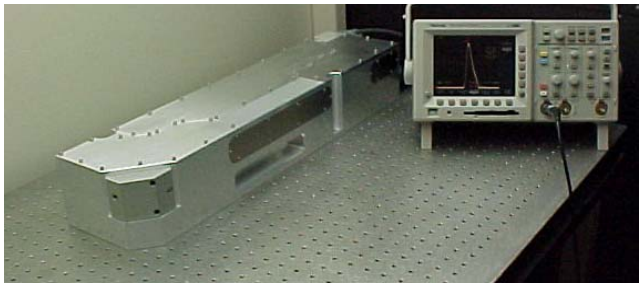

Figure 10: Photograph of next-generation high-power diode-pumped Q-switched intra-cavity frequency-converted 355 nm laser.

References

[1] W. Wiechmann" "Diode-Pumped Q-Switched 355-nm Lasers", Laser Technik Journal, September 2005, pp 35-37.

[2] M. Arbore, D. Balsley, J. Morehead, F. Adams, W. Wiechmann, J. Kmetec, Y. Zhou, and W. Grossman: "Measurement Techniques for Laser Parameters Relevant to Materials Processing", Proceedings of Photonics West, San Jose, California, USA, 2005, vol. 5713, pp 402-409.

[3] L. Eyres, J. Morehead, J. Gregg, D. Richard, and W. Grossman: "Advances in High Power Harmonic Generation: Q-Switched Lasers with Electronically Adjustable Pulse Width", Proceedings of Photonics West, San Jose, California, USA, 2006, vol. 6100, pp 349-358.

[4] J. E. Murray and S. E. Harris: "Pulse Lengthening via Overcoupled Internal Second-Harmonic Generation", J. Appl. Phys. 41, pp 609-613, 1970.

[5] J. Kmetec: U. S. Patent 5774488 (1998) (Patent).

[6] W. Grossman: U. S. Patent 5850407 (1998) (Patent).

(Received: May 16, 2006, Accepted: February 20, 2007)